International Immunology, Vol. 21, No. 2, pp. 123–135
doi:10.1093/intimm/dxn130

CD8β knockout mice mount normal anti-viral CD8+ T cell responses—but why?

Georgi S. Angelov, Philippe Guillaume and **Immanuel F. Luescher**

Ludwig Institute for Cancer Research, Lausanne Branch, University of Lausanne, 1066 Epalinges, Switzerland

Keywords: cell differentiation, cytotoxic T cells, TCRs, transgenic/knockout mice, viral infection

Abstract

It has been shown previously that CD8β *in vitro* increases the range and the sensitivity of antigen recognition and *in vivo* plays an important role in the thymic selection of CD8+ T cells. Consistent with this, we report here that CD8+ T cells from CD8β knockout (KO) P14 TCR transgenic mice proliferate inefficiently *in vitro*. In contrast to these findings, we also show that CD8β KO mice mount normal CD8 primary, secondary and memory responses to acute infection with lymphocytic choriomeningitis virus. Tetramer staining and cytotoxic experiments revealed a predominance of CD8-independent CTL in CD8β KO mice. The TCR repertoire, especially the one of the TCRα chain, was different in CD8β KO mice as compared with B6 mice. Our results indicate that in the absence of CD8β, CD8-independent TCRs are preferentially selected, which *in vivo* effectively compensates for the reduced co-receptor function of CD8αα.

Introduction

Thymus-derived CD8+ TCRαβ+ T cells typically express heterodimeric CD8αβ consisting of a disulfide-linked α and β chain (1). CD8 can also be expressed as homodimeric CD8αα, namely on intra-epithelial T lymphocytes, some dendritic cells, NK, NKT and TCRγδ+ T cells (2, 3). Both forms of CD8 bind to the non-polymorphic domain of MHC class Ia molecules and associate via CD8α with the intracellular Src tyrosine kinase $p56^{lck}$ (4). On murine T cells, CD8β cannot be surface expressed in the absence of CD8α (5). *In vitro* studies, mainly based on T cell hybridomas, have demonstrated that CD8β endows CD8 with efficient co-receptor function because it strengthens (i) the binding of MHC I–peptide to TCR, (ii) the association of CD8 with TCR, (iii) the partitioning of CD8 in lipid rafts and (iv) the association of CD8α with $p56^{lck}$ and the linker of activation of T cells (6–12).

In vivo, CD8β has been shown to play a critical role in thymic selection of CD8+ T cells; CD8β knockout (KO) mice have 3- to 5-fold lower numbers of mature CD8αα+ peripheral lymphocytes (13–15). In contrast to these findings, it has been reported that CD8β KO mice mount normal primary cytotoxic CD8 responses upon acute viral infections (14). Also cells from these mice exhibited normal cytotoxicity after *in vitro* stimulation with allogeneic splenocytes (13). Even CD8α KO mice were shown to contain acute and chromic viral infections (16, 17). In these mice, there was a strong bias to CD4+ T cells (13, 14, 16). However, even MHC class II-deficient CD8α KO mice produced good cytotoxic T cell responses upon acute infection with lymphocytic choriomeningitis virus (LCMV) (16). The objective of the present study was to elucidate why in these *in vivo* studies CD8β (and CD8α) was largely dispensable, while in previous *in vitro* studies, CD8β was found to greatly increase the sensitivity of antigen recognition by CD8+ T cells (6–12). These striking differences might be explained by mechanisms that compensate for the reduced co-receptor activity of CD8αα *in vivo*. For example, the functional avidity of CD8+ T cells has been reported to depend on changes in cell membrane lipid raft composition and on the arrangements of TCR and CD8 (18, 19). Alternatively, they could be explained by changes in the TCR repertoire. For example, the usage of TCR Vβ chains in naive CD8α KO and C57BL/6 (B6) mice has been shown to be significantly different (16, 17).

Furthermore, we wished to find out whether CD8β KO mice can generate normal CD8 memory and recall responses. Formation of primary effectors does not necessarily give rise to long-term functional CD8 memory (20, 21). Memory development is programmed during T cell–antigen presenting cell interaction and depends on the quality and duration of the original antigenic stimulus (22, 23, 24). Because CD8β affects TCR–MHC I–peptide interactions and TCR proximal signaling, it could also play a role in memory T cell formation. To address these questions, we used acute viral infections with LCMV, which elicit strong CD8 responses that have been extensively studied previously in B6 mice

Correspondence to: I. F. Luescher; E-mail: immanuel.luescher@licr.unil.ch

Received 6 August 2008, *accepted* 14 November 2008

Transmitting editor: T. Hünig

Advance Access publication 15 December 2008

(24, 25, 28). Major LCMV epitopes include the D^b-restricted GP33–41 (KAVYNFATC), nucleoprotein (NP)396–404 (FQPQNGQFI), GP276–306 (SGVENPGGYCL) and the K^b-restricted sub-dominant epitope NP205–212 (YTVKYPNL) (26–28). The GP33–41 peptides can also be presented and recognized in the context of K^b, although for optimal K^b presentation the sequences 34–41 or 34–42 are superior (26, 27). The Vα2+ and Vβ8.1+ P14 TCR recognizes GP33–41 in the context of D^b and is expressed in the P14 TCR transgenic (Tg) mouse (29).

We report that CD8β KO mice were able to generate strong anti-viral primary, secondary and memory CD8+ T cell responses. The poor co-receptor function of CD8αα was effectively compensated by selection and expansion of high avidity CD8-independent effector cells during LCMV infection.

Materials and methods

Mice and infections

Six-week-old C57BL/6 (B6) mice were purchased from Harlan (Horst, The Netherlands). CD8β KO mice were obtained from D. Littman and bred in the Institute's Animal Facility. To generate the P14 CD8β KO, P14 recombinase activating genes (RAG) KO, P14 CD8β KO RAG KO mice, P14 TCR transgenic and CD8β KO and/or RAG KO mice were crossed, intercrossed and the desired phenotype was conformed by simultaneous FACS analysis. Mice were infected intravenously (i.v.) with 200 PFU of LCMV strain WE (provided by C. Müller, University of Bern, Switzerland). Secondary GP33-specific responses were elicited by subcutaneous (s.c.) injection of 100 μg of GP33 peptide (KAVYNFATA)-conjugated virus-like particles (VLPs) (kindly provided by M. Bachmann, Cytos, Zürich). Recall responses at day 4 were analyzed in the draining axillary and brachial lymph nodes. Naive mice were infected intra-nasally with 50 PFU of PR8 influenza A virus under anesthesia with isoflurane. Primary CD8+ T cell responses were examined 10 days after infection. All experiments involving animals were approved by the Cantonal Veterinary Office (Lausanne, Switzerland).

In vivo and in vitro cytotoxicity assays

In vivo cytotoxicity assay was performed as described previously (30). Briefly, splenocytes from naive C57BL/6 mice were labeled with 1 or 0.1 μM of 5-(and-6)-carboxyfluorescein diacetate succinimidyl ester (CFSE, Molecular Probes, Eugene, OR, USA) and then pulsed with the indicated LCMV peptides (1 μM) and transferred i.v. (5×10^6 cells of each population) into groups of four mice each. Four hours later, lymphocytes were isolated from recipient's spleens. Labeled cells were distinguished from one another based on their different CFSE staining. The percent killing was calculated as follows: 1 − [({percentage of peptide pulsed in infected/ percentage of unpulsed in infected}/{percentage of peptide pulsed in uninfected/ percentage of unpulsed in uninfected}) × 100]. For *in vitro* cytotoxicity assay, ^{51}Cr-labeled, D^b-transfected P815 cells (5×10^3 cells per well) were incubated for 30 min at 37°C with the indicated concentrations of GP33 (KAVYNFATA) peptide. After washing, target cells were incubated with splenocytes from LCMV-infected [8 days (d8)] CD8β KO or B6 mice, in presence or absence of 5 μg of anti-CD8α antibody (53-6.72). The effector to target cell ratio was adjusted to 30/1, considering as effectors D^b loaded with GP33 peptide (D^b-GP33) tetramer-positive splenocytes. After 4 h of incubation at 37°C, released ^{51}Cr was determined and the specific lysis calculated as follows: 100 × [(experimental − spontaneous release)/(total − spontaneous release)].

Antibodies and tetramers

Production and binding studies with tetramers were performed essentially as described previously (30). Briefly, LCMV effector or memory cells were incubated at 4°C for 60 min in FACS buffer (PBS supplemented with 1% FCS and 0.01% sodium azide) with 50 nM or the indicated concentrations of D^b-GP33 or CD8-binding deficient D^b Q226A, D227K-GP33 tetramers (31). The following fluorescent anti-mouse mAbs were purchased from BD Biosciences: anti-CD8α (53-6.72), anti-IFN-γ (XMG1.2), anti-CD44 (IM7), anti-CD62L (MEL-14), anti-CD122 (TM-b1), anti-CD127 (SB/199), anti-CD4 (GK1.5), anti-TCR Vβ antibodies Vβ 2, 3, 4, 5.1/2, 6, 7, 8.1/2, 8.2, 8.3, 9, 10, 11, 12, 13 and 14 and anti-TCR Vα antibodies Vα 2, 3.1, 8 and 11.

Intracellular cytokine staining and peptides

Spleen or lymph node cells (3×10^6) were incubated in 96-well round-bottom plates with 0.67 μl ml^{-1} of GolgiStop (BD Biosciences) in the presence or absence of 100 nM or the indicated concentrations of the LCMV peptides GP33 (KAVYNFATA), NP396 (FQPQNGQFI), GP276 (SGVENPGGYCL) and NP205 (YTVKYPNL) for 6 h at 37°C. Cells were then permeabilized by incubation for 20 min in Cytofix–Cytoperm solution (BD Biosciences) and stained with anti-IFN-γ antibody following the manufacturer's instructions.

In vitro proliferation assay

Lymph node and spleen cells from P14 RAG KO or P14 CD8β KO RAG KO TCR transgenic mice were pooled and incubated at 3×10^7 cells ml^{-1} with 10 μM CFSE (Molecular Probes) at 37°C for 10 min. Cells were then washed once with ice-cold DMEM (Invitrogen Life Technologies) containing 5% FCS, followed by two more washes in PBS. CFSE-labeled cells were incubated with irradiated syngeneic B6 splenocytes previously pulsed (1 h at 37°C) with indicated concentrations of GP33 (KAVYNFATA) or Y4A (KAVANFATA) peptides. Proliferation was assessed by flow cytometry 72 h after the stimulation.

Results

Primary anti-LCMV responses in CD8β KO mice

To examine CD8+ T cell's ability to generate effector functions in the absence of CD8β, we compared LCMV-specific responses d8 after acute LCMV infection in CD8β KO and B6 mice. The frequencies of IFN-γ-producing splenocytes from CD8β KO overall was comparable upon *ex vivo* stimulation with 100 nM of the D^b-restricted GP33, NP396, GP276 and the K^b-restricted NP205 peptides to those from B6 mice, although there were differences among the four epitopes (Fig. 1A). Because GP33–41 peptides can also bind to

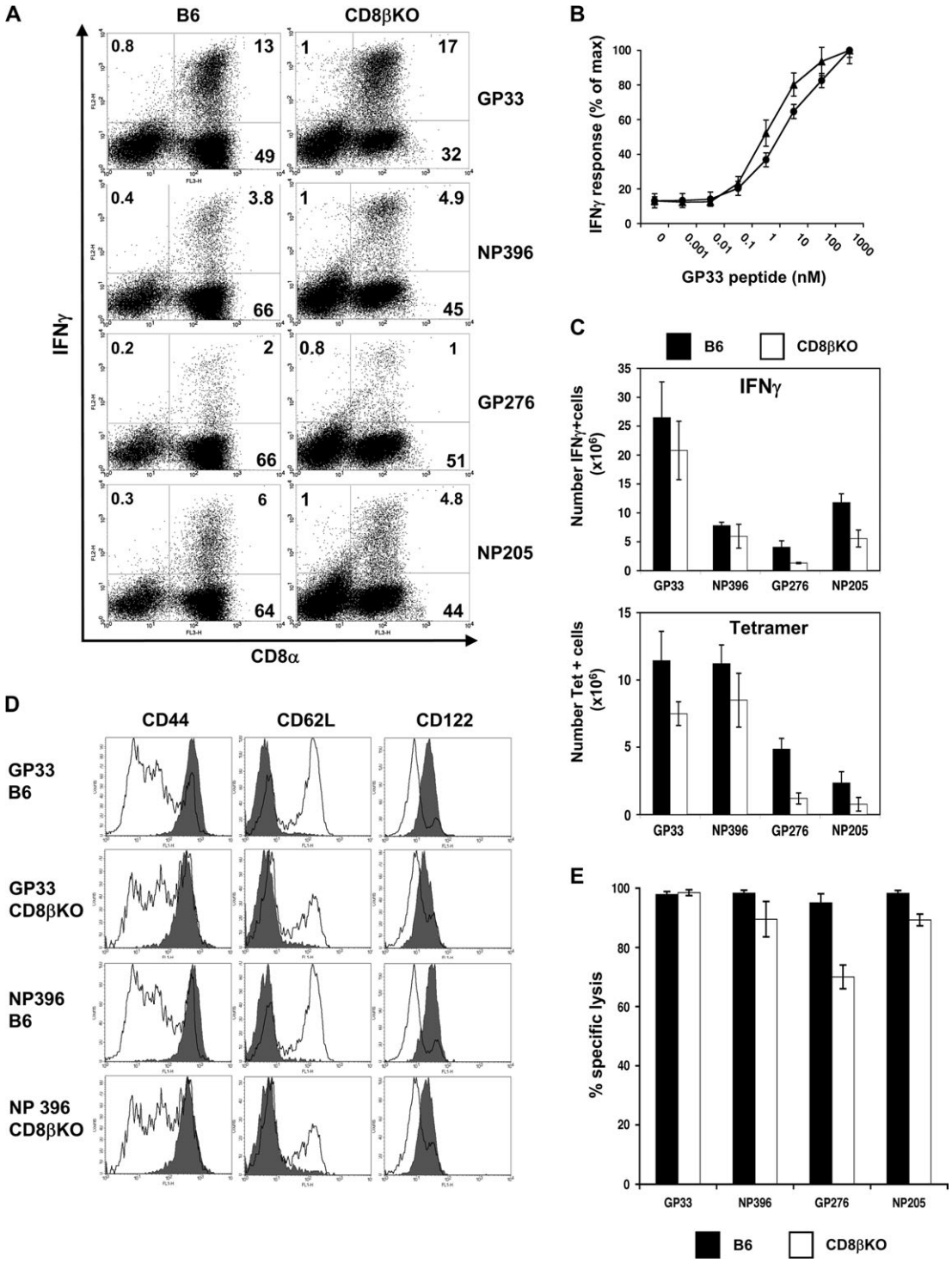

Fig. 1. CD8β KO mice mount efficient primary anti-LCMV response. (A) IFN-γ production of CD8+ splenocytes pooled from four B6 and CD8β KO mice, respectively, on day 8 after LCMV infection was determined after *ex vivo* stimulation with 100 nM of indicated LCMV peptides. The percentage of splenocytes in the lymphocyte/lymphoblast gate is shown for each of the quadrants. (B) The splenocytes from B6 (triangles) or CD8β KO mice (circles) were incubated with P815-D^b cells that were previously pulsed with the indicated concentrations of GP33–41 peptides, and the intracellular IFN-γ expression was assessed likewise. Mean values and standard deviations (SDs) were calculated from three experiments. (C) Total numbers of IFN-γ-producing and tetramer-binding CD8 effector cells in B6 (solid bars) or CD8β KO mice (open bars). Mean values and SDs were calculated from four individual mice per group from one of three experiments. (D) Phenotypic analysis of D^b-GP33 and D^b-NP396 tetramer-positive CD8 T cells. Filled histograms are gated on either GP33- or NP396-positive effector cells. Open histograms indicate naive cells. (E) *In vivo* cytotoxic function of effector CD8+ T cells. CFSE-labeled target cells loaded with the indicated LCMV peptides were transferred into B6 (black bars) or CD8β KO mice (open bars) d8 post-LCMV infection. Specific lysis in the spleens was determined 4 h later. One of three experiments with mean values and SDs of four mice per group is shown. The *P*-values were calculated using two-sided Student's *t*-test.

and be recognized in the context of K^b (26, 27), we assessed the IFN-γ response of the splenocytes following incubations with P815 cells (H-2^d) transfected with D^b (P815-D^b) and pulsed with graded concentrations of GP33 peptide. The IFN-γ response of B6 splenocytes was slightly higher in the range of 1–100 nM peptide as compared with CD8β KO cells (Fig. 1B). Because the inverse was true when using 100 nM of GP33–41 peptides in autologous presentation (Fig. 1A), a part of this IFN-γ response was indeed K^b restricted. This experiment also shows that differences in the IFN-γ response were scant over a wide range of peptide concentrations.

The total numbers of IFN-γ-producing splenocytes from CD8β KO mice overall were lower as compared with cells from B6 mice (Fig. 1C). For the epitopes NP276 and NP205, the numbers of IFN-γ-producing cells were 2- to 3-fold lower, but <2-fold lower for the NP396 and GP33 determinates. The total numbers of tetramer-positive cells were also lower in CD8β KO mice than in B6 mice. In the spleens of naive CD8β KO mice, CD8α+ T cells were ~3% and in B6 spleens 9%. Eight days after infection, the former expanded to ~36% and the latter to ~62%. Thus, on a per cell basis, the CD8+ T cells from CD8β KO mice exhibited at least as strong IFN-γ responses as cells from B6 mice. Statistically, this is particularly significant for the GP276 and NP205 responses. At the peak of the LCMV infection, the expression of CD44, CD122 and CD62L was essentially the same in CD8β KO and B6 mice (Fig. 1D). Similar results were obtained when examining acute infections with influenza PR8. The proportions and total numbers of IFN-γ-producing, D^b-restricted, NP366-specific effector cells in bronchoalveolar lavages at the peak of the primary influenza response (day 10) were similar in B6 and CD8β KO mice (data not shown).

Eight days after LCMV infection, peptide-loaded target cells were lysed nearly as efficiently in CD8β KO as in B6 mice (Fig. 1E). The modest reduction in killing in the case of NP276 was with high statistical significance smaller than the difference in the numbers of NP276 tetramer-specific cells (Fig. 1C). This was also true in NP205 and with lesser statistical significance for NP396. Thus, CD8β-deficient effector cells clearly displayed unimpaired, if not increased, cytotoxicity *in vivo*. Taken collectively, these results indicate that the differentiation of functional effector cells was altered in subtle ways, but overall not impaired in CD8β KO mice. Our results are in accordance with the observation that splenocytes from LCMV- or vesicular stomatitis virus (VSV)-infected CD8β KO mice at the peak of the acute infection displayed *ex vivo* nearly the same anti-GP33 LCMV and anti-VSV cytotoxic responses as splenocytes from B6 mice (14).

LCMV infection in CD8β KO mice elicits long-term functional CD8 memory

We next investigated the development of CD8 memory in CD8β KO mice. Their spleens were analyzed for virus-specific memory CD8+ T cells 3 months after LCMV infection. As assessed by intracellular IFN-γ staining upon *ex vivo* stimulation with 100 nM peptide, slightly higher frequencies of GP33- and NP396-specific memory cells were found in CD8β KO mice than in B6 mice (Fig. 2A). This was also true when lower peptide concentrations were used for stimulation (data not shown). Conversely, for the GP276 and NP205 epitopes, the frequencies of IFN-γ-responding memory cells were ~2-fold lower. The total numbers of IFN-γ-producing cells in CD8β KO mice were equal or higher for the GP33 and NP396 and lower for the GP276 and NP205 epitopes (Fig. 2B), whereas the total number of tetramer-positive splenocytes was lower in CD8β KO mice for all epitopes (Fig. 2B). These differences were statistically most significant for the GP276 and NP205 epitopes. The percentage of CD8+ splenocytes was ~18% for CD8β KO and B6 mice, but the absolute number was lower for CD8β KO mice (~1.2×10^7 versus 2.8×10^7 cells per spleen). Thus, on a per cell basis, the IFN-γ response of CD8+ memory cells from CD8β KO mice was superior as compared with B6 mice. Consistent with this, we found that CD8β KO mice efficiently cleared LCMV, even when 10 times higher viral loads were used (Supplementary Figure S1, available at *International Immunology* Online).

To further characterize the LCMV-specific CD8+ splenocytes, we examined the expression of cell surface markers that characterize memory CD8+ T cells. CD44, CD122 and CD127 were equally up-regulated on tetramer-positive cells from CD8β KO and B6 mice (Fig. 2C). The up-regulation of the cytokine receptor chains CD122 and CD127 is a hallmark of long-term memory CD8+ T cells and was not affected by CD8β deficiency [Fig. 2C and (32)]. Memory cells typically exhibit heterogeneous CD62L expression, corresponding to central and effector memory cell subsets, which was observed both on cells from CD8β KO and B6 mice. Both memory subsets were present at similar proportions in CD8β KO and wild-type (WT) mice [Fig. 2C and (33)].

Another characteristic of CD8 memory T cells is their rapid *in vivo* cytotoxicity (34). Memory CD8β KO cells exhibited 15–30% higher *in vivo* killing of autologous targets sensitized with each of the four LCMV epitopes (Fig. 2D). Since the total numbers of the LCMV epitope-specific memory cells were lower in CD8β KO mice, this argues they had higher cytotoxicity than those of B6 mice. Taken together, these results demonstrate that the absence of CD8β did not impair the differentiation in and the functional integrity of long-lived memory CD8+ T cells following acute LCMV infection.

A hallmark of memory T cells is to mount rapid and strong recall responses. We therefore examined the recall responses 2 months after acute LCMV infection. To avoid interference by neutralizing antibodies, we used VLPs conjugated with the GP33 peptide (KAVYNFATA) to elicit GP33-specific recall responses (35). Four days after s.c. challenge with GP33-VLPs, the IFN-γ response was measured in the draining lymph nodes. Higher proportions and absolute numbers of IFN-γ-producing CD8+ T cells as well as D^b-GP33 tetramer-positive cells were found in the lymph nodes of CD8β KO (Fig. 3A and B). This was explained, at least in part, by the higher initial number of GP33-specific memory cells in the lymph nodes of CD8β KO mice (Fig. 3B). The relative expansion of IFN-γ-producing and of D^b-GP33 tetramer-binding cells of the recall response was similar in CD8β KO and B6 mice (Fig. 3C). GP33-VLPs also elicited primary anti-GP33 epitope-specific responses that were similar

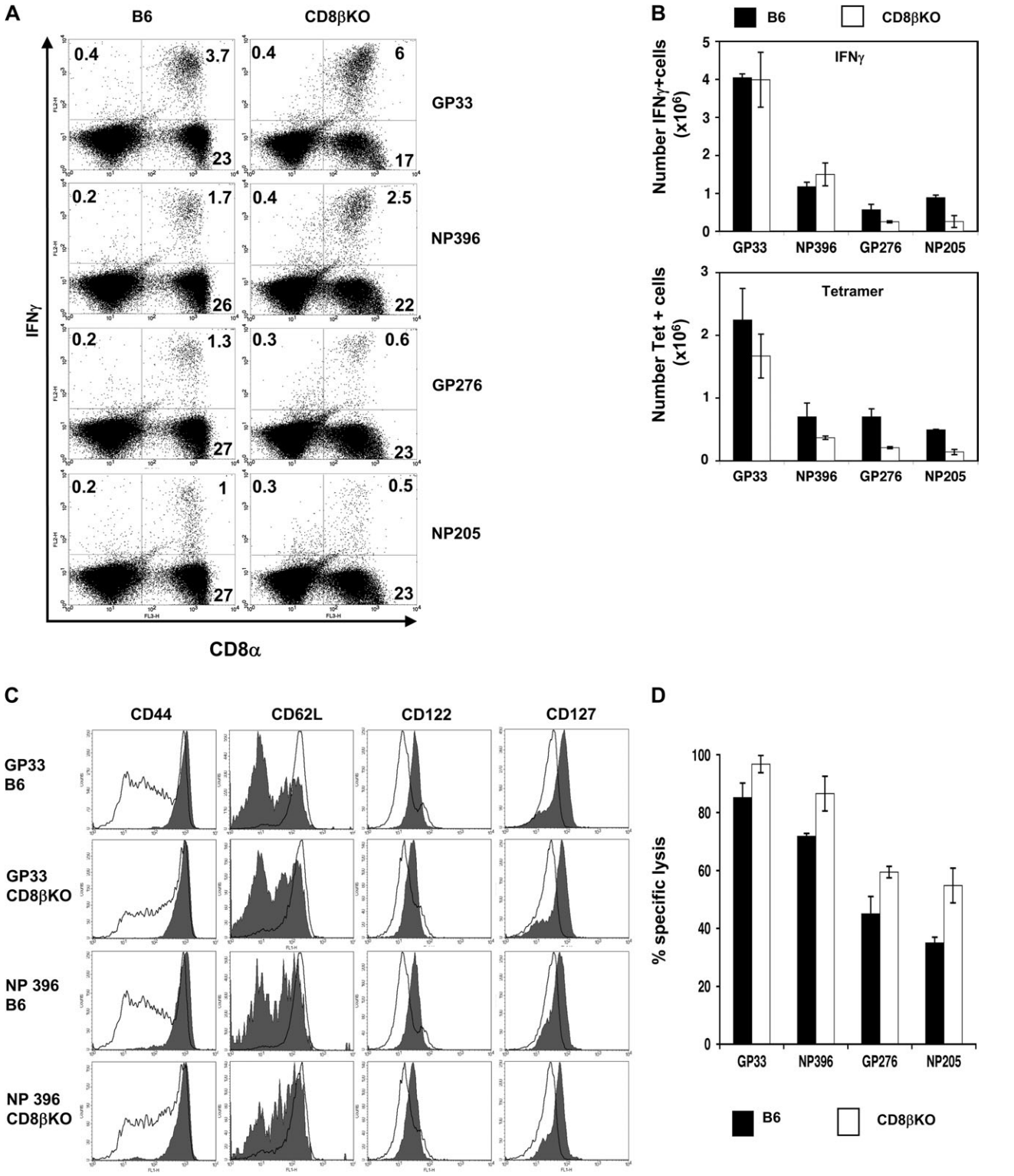

Fig. 2. CD8β KO mice form stable anti-LCMV memory CD8 T cells. (A) Percentages of IFN-γ-producing memory CD8 T cells in the spleens 90 days after LCMV infection upon *ex vivo* stimulation with 100 nM of the indicated peptides. One representative experiment is shown. (B) Total numbers of IFN-γ-positive and tetramer-specific CD8+ T cells in the spleens of LCMV immune mice. Bars represent mean values from three mice per group from one representative experiment out of four. (C) *Ex vivo* phenotypic analysis of GP33 and NP396 tetramer-specific memory CD8 T cells. Histograms are gated on either GP33- or NP396-specific memory CD8+ T cells. Open histograms indicate naive cells. (D) *In vivo* cytotoxic function of memory CD8+ T cells. CFSE-labeled targets loaded with indicated LCMV peptides were transferred into B6 (black bars) or CD8β KO mice (open bars) 103 days post-LCMV infection. Specific lysis in the spleens was determined 4 h later. One experiment with mean values and standard deviations of four mice per group is shown. Results were reproduced in two separate experiments. The *P*-values were calculated using two-sided Student's *t*-test.

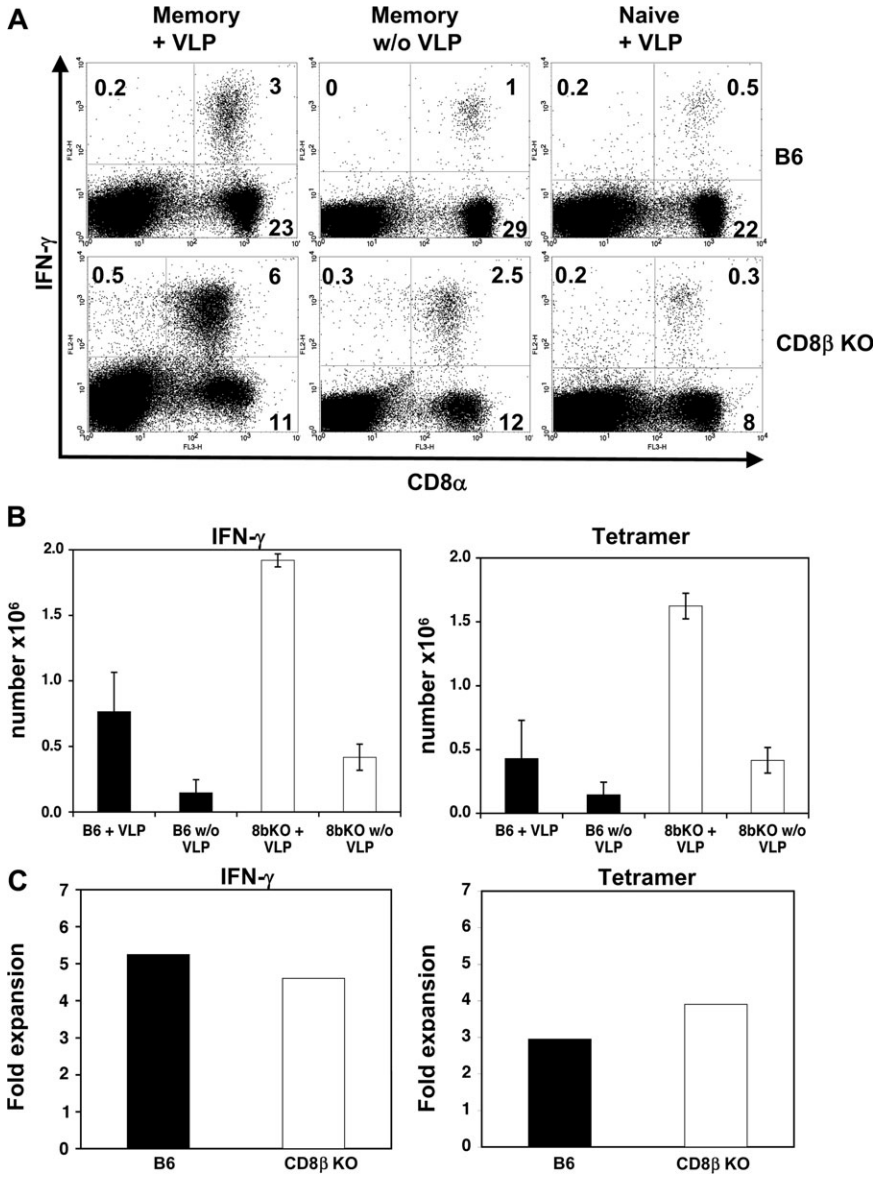

Fig. 3. CD8β KO mice generate strong secondary anti-GP33 response. Naive or LCMV immune (day 60 post infection) mice were injected s.c. with GP33 peptide containing VLPs and the response was analyzed 4 days later in draining axillary and brachial lymph nodes. (A) The percentages of IFN-γ-producing cells in the lymphocyte/lymphoblast gate are shown for each of the quadrants. (B) Average numbers of tetramer-positive and IFN-γ-producing cells in draining lymph nodes of VLP-challenged B6 (black bars) or CD8β KO (open bars) mice were calculated from four individual mice. Results were reproduced in two experiments with four mice per group. (C) The fold expansion corresponds to the ratio between the average numbers for tetramer-positive or IFN-γ-producing cells in GP33-VLP-challenged versus non-challenged memory mice. The *P*-values for the indicated groups were calculated using two-sided Student's *t*-test.

in CD8β KO and B6 mice (Fig. 3A). Strong secondary GP33-specific responses were also observed when CD8+ memory cells from CD8β KO mice were transferred into B6 mice, which were then infected with LCMV (data not shown). Interestingly, in the spleens, the frequency of GP33-specific CD8+ T cells was higher in B6 than in CD8β KO mice, while in the lymph nodes, the inverse was true (Figs 1–3 and data not shown). Taken collectively, these results demonstrate that the long-lived memory CD8+ T cells in CD8β KO mice were capable to efficiently expand and to produce IFN-γ upon challenge by GP33-VLPs or by LCMV infection.

GP33-specific CTL from CD8β KO mice are CD8 independent

The findings that CD8β is dispensable for CD8 T cell responses *in vivo* is at odds with previous *in vitro* studies, indicating that CD8β broadens the range and increases the sensitivity of antigen recognition (6–12). To investigate this divergence, we assessed the cytolytic activity of splenocytes from CD8β KO and B6 mice d8 after LCMV infection. Cells from B6 mice efficiently killed sensitized P815-D^b targets (Fig. 4A). Half-maximal lysis was slightly below 10^{-10} M GP33 peptide. By contrast, CD8-binding deficient P815-D^b226/227 targets were killed inefficiently and half-maximal

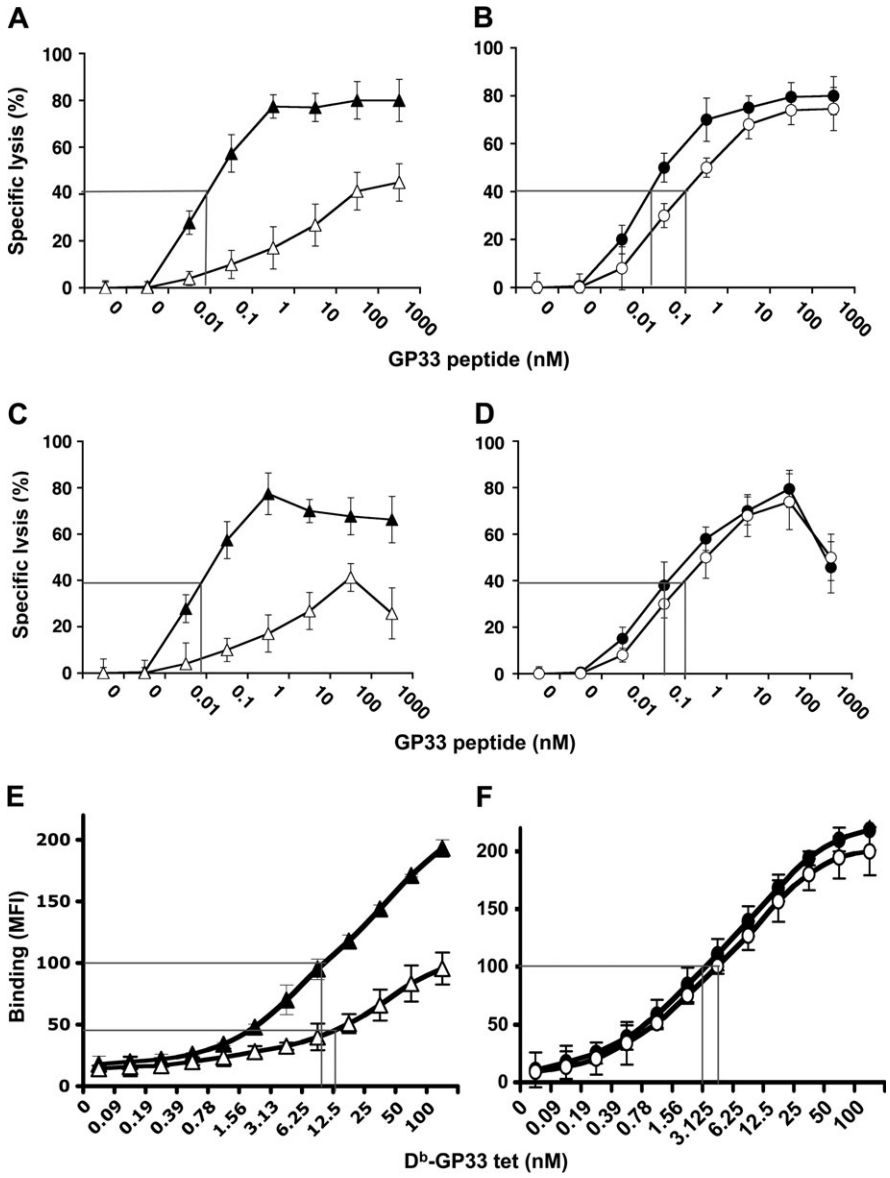

Fig. 4. D^b-GP33-specific CTL from CD8β KO mice are CD8 independent. (A–B) Splenocytes from day 8 LCMV-infected B6 (triangles) or CD8β KO (circles) mice were incubated with P815-D^b (filled symbols) or P815-D^b226/227 cells (open symbols) previously pulsed with the indicated concentrations of GP33–41 peptides. Mean values were calculated from triplicates. (C–D) Alternatively, the experiment was performed using only GP33-pulsed P815-D^b targets in the presence (open symbols) or absence (filled symbols) of anti-CD8α mAb 53.6.72. (E–F) Splenocytes from day 8 LCMV-infected B6 (triangles) or CD8β KO (circles) mice were incubated at 4°C with the indicated concentrations of D^b/GP33–41 (filled symbols) or D^b226/227-GP33–41 tetramers (open symbols) and the binding was determined. Mean values and standard deviations of three mice per group from one experiment out of three are shown.

lysis required an ~100-fold higher peptide concentration (Fig. 4A). Conversely, splenocytes from CD8β KO mice killed P815-D^b targets as efficiently as splenocytes from B6 mice, and half-maximal lysis required only slightly higher peptide concentration (Fig. 4B). Remarkably, however, CD8β KO splenocytes killed P815-D^b226/227 targets nearly as efficiently as P815-D^b targets. Essentially, the same results were obtained when P815-D^b targets were used in the absence or presence of the CD8α-blocking antibody 53.6.72 (Fig. 4C and D). Taken together, these results demonstrate that the cytotoxic response of GP33-specific CTL from CD8β KO mice was CD8 independent, whereas the one from B6 mice was CD8 dependent.

We next examined the binding of D^b-GP33–41 and D^b mutant at residues 226 and 227 loaded with GP33 peptide (D^b226/227-GP33)–41 tetramers to splenocytes from CD8β KO and B6 mice d8 after LCMV infection. D^b-GP33 tetramer bound to CD8β KO splenocytes more efficiently than to B6 splenocytes (Fig. 4E and F). The higher maximal binding on CD8β KO splenocytes may be explained, at least in part, by the fact that GP33-specific splenocytes from CD8β KO mice expressed more TCRs than those B6 mice (mean

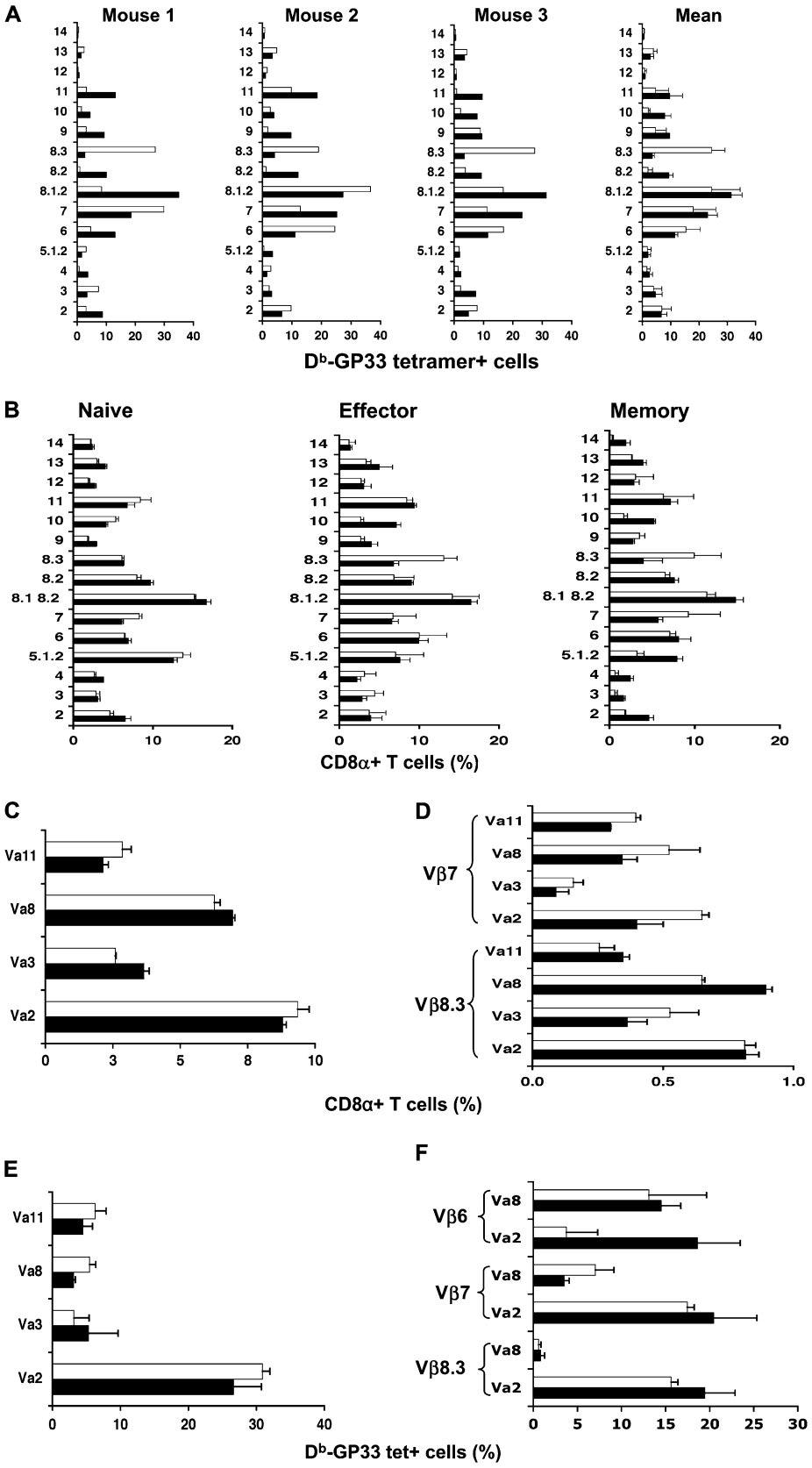

Fig. 5. CD8β KO mice exhibit different TCR repertoires than B6 mice. (A) CD8α+ splenocytes from d8 LCMV-infected B6 (black bars) or CD8β KO mice (open bars) were stained with the indicated anti-Vβ mAb and D^b-GP33–41 tetramer (50 nM) and analyzed by flow cytometry.

fluorescence intensity after staining with PE-labeled anti-TCR mAb H57 was 1419 versus 1192). Half-maximal binding of D^b-GP33 tetramer to cells from CD8β KO mice required about four times lower concentration as compared with cells from B6 mice. Remarkably, while the D^b226/227-GP33–41 tetramer bound to CD8β KO cells nearly as efficiently as the D^b-GP33 tetramer, it very poorly stained B6 splenocytes (Fig. 4E). Taken collectively, these results indicate that GP33-specific CD8+ effector cells from CD8β KO mice are CD8 independent in terms of target cell killing and tetramer binding, whereas those from B6 mice rely for both on CD8 co-engagement.

CD8β deficiency alters the TCR repertoire

We next examined whether the difference in CD8 dependence of GP33-specific CTL in B6 and CD8β KO splenocytes was related to differences in the TCR repertoire. First, we assessed the TCR Vβ usage of D^b-GP33 tetramer+ CD8+ T cells by means of anti-Vβ mAb and flow cytometry. Eight days after LCMV infection, tetramer+ splenocytes from CD8β KO mice exhibited a nearly 10-fold higher percentage of Vβ8.3+ T cells than those from B6 mice (Fig. 5A). Smaller differences were observed for other Vβ. For example, Vβ6+ T cells were slightly more frequent in the spleens of CD8β KO mice as compared with those of B6 mice. The inverse was true for Vβ 7, 8.1, 8.2, 9, 10 and 11+ cells. These differences were also visible on total CD8α+ T cells from d8 LCMV immune mice, albeit less pronounced and with low statistical significance (Fig. 5B). This is expected because the CD8 response to acute anti-LCMV infection is highly diverse and the D^b-GP33-specific response constitutes only a fraction (26). The same analysis performed on d80 LCMV immune cells showed the same and additional differences, such as significant skewing of the usage of Vβ5.1.2 and Vβ7. By contrast, in total CD8α+ T cells no marked differences in Vβ usage were noticed between CD8β KO mice and B6 mice (Fig. 5B).

We then performed the same analysis with anti-Vα-specific mAb, which was limited, because only four antibodies were available. On the total CD8α+ T cells from naive B6 and CD8β KO mice, the proportion of Vα2+ cells was remarkably high (9–10%), followed by Vα8 (6–7%). The differences in the usage of Vα2, Vα3.2, Vα8 and Vα11.2 were statistically significant, but modest (10–20%) (Fig. 5C). To find out whether differences were obscured by high diversity, we repeated this experiment by gating on CD8α+ T cells expressing Vβ7 or 8.3. Clear differences between B6 and CD8β KO mice thus became visible. For example, in CD8+ splenocytes from CD8β KO, Vβ7+ T cells expressed 30–40% more Vα2 ($P = 0.02$) and Vα8 ($P = 0.08$), whereas Vβ8.3 splenocytes exhibited more Vα8 ($P = 0.0001$).

A similar scenario was observed when analyzing D^b-GP33-specific CD8α+ T cells from d8 LCMV immune mice. D^b-GP33+ CD8α+ T cells from CD8β KO and B6 mice expressed 26–30% Vα2, but only 3–7% of Vα3.2, Vα8 and Vα11.2 (Fig. 5E). The differences in expression of these Vα between CD8β KO and B6 cells were small and statistically barely significant. Again, considerably larger differences were seen when the D^b-GP33 tetramer+ cells were gated on Vβ6-, 7- or 8.3-expressing cells (Fig. 5F). For example, Vβ6+ cells from B6 mice expressed about five times more Vα2 than cells from CD8β KO mice ($P = 0.013$). Similarly, Vβ8.3+ cells from B6 mice expressed nearly 2-fold more Vα2 than cells from CD8β KO mice ($P = 0.003$) and Vβ7+ from B6 mice two times less Vα8 than cells from CD8β KO mice ($P = 0.02$). Taken together, these results demonstrate that there are clear and statistically significant differences in the TCR repertoire in B6 versus CD8β KO mice. For the TCRβ chains, differences in Vβ usage were notable only on CD8+ effector and memory cells and especially on D^b-GP33-specific CTL. For the TCRα chains, statistically significant differences in Vα usage were seen on naive as well as on D^b-GP33-specific effector cells only when gating on subpopulations expressing given Vβ, which suggests highly diverse TCRα chain repertoires in both mice.

In order to assess the role of CD8β in a setting where only one defined TCR is available, we crossed CD8β KO and P14 TCR Tg mice. As reported previously, splenocytes and lymph node cells from P14 TCR Tg mice were predominantly D^b-GP33 tetramer+ (97%) and expressed the Tg Vα2+ TCRα chain and the Vβ8.1+ TCRβ chain [Fig. 6A and (29)]. Remarkably, CD8β-deficient P14 TCR Tg mice (P14 × CD8β KO) predominately expressed also the Tg Vβ8.1 TCRβ chain, but variable levels of the Vα2+ Tg TCRα chain. The expression of Vα2 and D^b-GP33 tetramer staining correlated, arguing that in P14 × CD8β KO mice diverse endogenous TCRα chains were co-expressed at various levels with the Tg P14 TCRα chain and that the tetramer binding was mediated primarily by the Tg P14 TCR. Moreover, in striking contrast to P14 TCR Tg mice, in P14 × CD8β KO mice nearly half of the D^b-GP33 tetramer+ cells were CD4+ (Fig. 6A and B). The total number of CD8+ lymph node cells in P14 mice was ~2-fold higher than in P14 × CD8β KO, i.e. a smaller difference when compared with B6 and CD8β KO mice (Supplementary Figure S2A, available at *International Immunology* Online). The total cell numbers in lymph nodes (and spleen) were comparable in P14 and P14 × CD8β KO, which is to a large extent explained by compensatory

The percentages of D^b-GP33 tetramer-positive cells recognized by the indicated anti-Vβ antibodies are shown. The right side panels indicate the mean values and standard deviations (SDs) of the three mice analyzed per group. (B) Groups of three B6 (black bars) or CD8β KO mice (open bars) were infected or not (naive) with LCMV and d8 (effector) or 80 days later (memory) their splenocytes were stained with anti-CD8α mAb 53.6.72 and the indicated anti-Vβ antibodies. The percentages of CD8α-positive cells recognized by the indicated anti-Vβ antibodies are shown. The mean values and SDs were calculated from three mice per group. (C) The same analysis was performed as described in (A) was performed using the indicated Vα antibodies. Mean values and SDs were calculated from three mice per group. (D) As in (C), but after gating on Vβ7 and Vβ8.3+ cells, respectively. (E) Splenocytes from d8 LCMV-infected B6 (black bars) or CD8β KO mice (open bars) were stained with D^b-GP33–41 tetramer and the indicated Vα antibodies. Shown are the percentages of tetramer+ expressing the respective Vα. Mean values and SDs were calculated from three mice per group. (F) As in (E), but after gating on anti-Vβ6, 7 or 8.3+ cells. The *P*-values refer to pairs of values for B6-derived and the corresponding CD8β KO-derived cells and were calculated using two-sided Student's *t*-test.

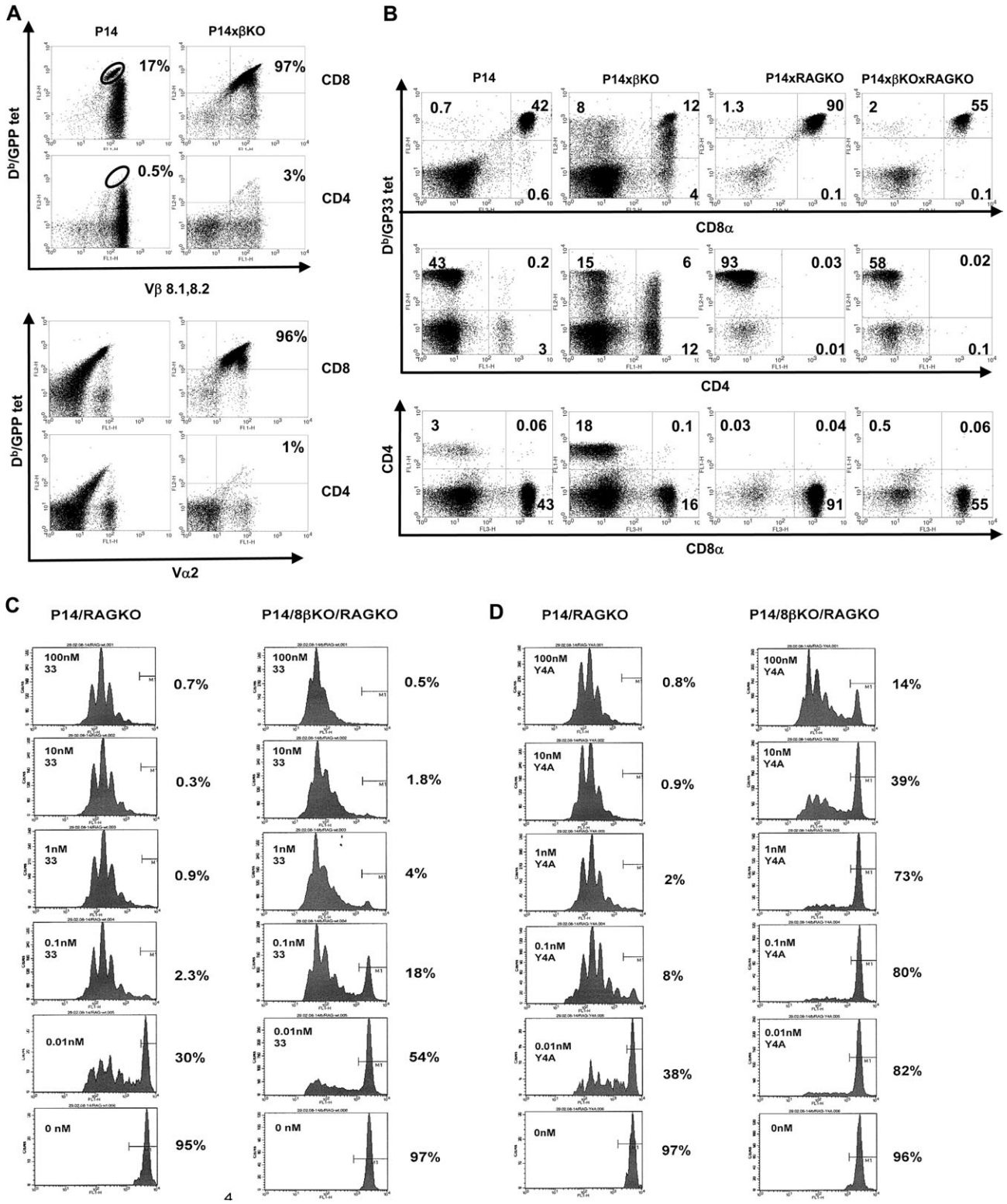

Fig. 6. CD8β affects the TCRα chain rearrangement and the proliferation of CD8+ cells from P14 TCR Tg mice. (A) Lymph node cells from P14 TCR Tg (P14) and from CD8β-deficient P14 TCR Tg mice (P14 × β KO) mice were stained as indicated with D^b-GP33–41 tetramer and antibodies specific for the P14 TCRα chain (Vα2) and β chain (Vβ8.1, 8.2), CD4 or CD8α and analyzed by flow cytometry, gating either on CD8α+ or on CD4+ cells. (B) Lymph node cells from P14 TCR Tg (P14), RAG-deficient P14 TCR Tg (P14 × RAG KO), CD8β-deficient P14 TCR Tg mice (P14 × β KO) or RAG- and CD8β-deficient P14 TCR Tg mice (P14 × β KO × RAG KO) were stained as indicated with D^b-GP33–41 tetramer and antibodies specific for CD8α and CD4, respectively, and analyzed by flow cytometry. The numbers indicate the percentages of cells in the respective quadrants or indicated domains. (C) Equal numbers of CFSE-labeled splenocytes from RAG-deficient P14 TCR Tg and P14 TCR Tg × CD8β KO

expression of CD4+ T cells (Supplementary Figure S2A and B, available at *International Immunology* Online).

When the P14 × CD8β KO mice were bred to RAG KO animals (P14 × CD8β KO × RAG KO), these CD4 cells disappeared (Fig. 6B). They also disappeared when P14 × CD8β KO mice were bred on MHC class II KO (data not shown). Moreover, cells from P14 × CD8β KO × RAG KO mice expressed only the Tg P14 TCR (Fig. 6A and B). These findings indicate that in P14 × CD8β KO, but not in P14 TCR Tg mice, endogenous TCRα chains are extensively rearranged.

CD8β promotes the proliferation of CD8α+ T cells from P14 TCR Tg mice

To assess the role of CD8β in the activation of cells expressing only one TCR, we assessed the *in vitro* proliferation of splenocytes from RAG-deficient P14 TCR Tg and P14 × CD8β KO mice. As assessed by CFSE labeling, 72 h after incubation with graded concentrations of GP33–41 peptides, the proliferation of CD8β-deficient cells exhibited impaired proliferation, especially at low peptide concentrations (Fig. 6C). The difference became striking, when the weak agonist peptide GP33–41 Y4A was used for stimulation. While the cells from P14 TCR Tg mice efficiently proliferated already at 0.1 nM, CD8β-deficient cells significantly proliferated only at >100 nM peptide (Fig. 6D). These results are consistent with the reported ability of CD8β to increase the range and the sensitivity of antigen recognition (6–12) and argue that the remarkably efficient anti-viral responses in CD8β KO mice are related to changes in the TCR repertoire.

Discussion

The present study provides detailed evidence demonstrating that CD8β KO mice upon acute LCMV infection mount primary CD8+ T cell responses that overall are equivalent to those of B6 mice (Fig. 1). This is in accordance with a previous study showing that CD8β KO mice generate normal cytotoxic responses upon acute infection with LCMV and VSV (14). Our study further indicates that the numbers of total and LCMV epitope-specific CD8α+ splenocytes from infected CD8β KO mice were significantly lower as compared with those from B6 mice (Fig. 1A). This demonstrates that on a per cell basis, the anti-LCMV-specific cells from CD8β KO mice were actually more reactive than those from B6 mice. Even CD8α KO mice have been shown to mount efficient primary T cell responses upon infection with LCMV and polyoma virus, respectively (16, 17). In addition, our study shows for the first time that CD8β KO mice also form long-lasting, functional CD8 memory and recall responses, indicating that *in vivo* CD8β is dispensable for the differentiation of bona fide CD8 memory cells, as well as their activation *in vivo* and *in vitro*. (Figs 2 and 3, G. S. Angelov and I. F. Luescher, unpublished results).

These findings are at variance with numerous previous *in vitro* studies demonstrating that CD8β increases the sensitivity and the range of antigen recognition (6–12). Our observation that splenocytes from CD8β-deficient P14 TCR Tg mice proliferated far less well than those from P14 TCR Tg mice is consistent with these studies. A key difference between these two sets of studies is that in the former strong polyclonal CD8+ T cell responses were investigated and in the latter monoclonal T cell responses. Although we cannot rule out that there may be compensatory mechanisms that allow CD8α+ T cells to adapt for the lesser co-receptor activity of CD8αα *in vivo*, several observations argue that these divergent findings are primarily explained by differences in T cell specificities. (i) There were subtle, but significant, differences in the anti-viral CD8 responses in B6 and CD8β (and CD8α) KO mice when analyzing different epitopes (Figs 1 and 2, unpublished results and 16, 17). This argues against putative compensatory mechanisms, which one would expect not to be epitope specific. (ii) There were clear differences in the repertoire of TCRβ chains in virus-infected B6, CD8β (and CD8α) KO mice (Fig. 5A and B and 16, 17). (iii) In virus-infected CD8β (and CD8α) KO mice, CD8-independent CTL were clearly dominant. For example, target cell killing by GP33-specific CTL from B6 mice was severely inhibited by blocking anti-CD8 antibodies or by CD8-binding ablating mutations of D^b, whereas those from CD8β KO mice were not (Fig. 4A–D). The CD8-independent nature of the CTL from CD8β KO mice was also evident from our tetramer-binding studies, showing that GP33-specific CTL from CD8β KO mice bound D^b226/227-GP33 tetramer as efficiently as D^b-GP33 tetramer, whereas CTL from B6 mice efficiently bound only the latter tetramer (Fig. 4E and F).

It is interesting to note that D^b-GP33 tetramer bound to splenocytes from d8 LCMV-infected mice from CD8β and CD8α KO mice more avidly than to cells from B6 mice [Fig. 4E and F and ref. (16)]. This is consistent with the prevailing view that CD8-independent TCRs typically have high affinity and hence can efficiently bind cognate MHC I–peptide complexes also without the avidity-enhancing effect of CD8 (36). It should be noted, however, that the differences in functional (i.e. half-maximal lysis) and physical avidity (i.e. D^b-GP33 tetramer binding) between GP33-specific CTL from B6 and CD8β KO mice are modest. More striking differences were observed when CD8-binding deficient target cells and tetramers were used (Fig. 4), indicating that CTL from CD8β KO mice in addition to having an increased avidity also are less CD8 dependent. It has been shown that CD8 dependence can be an intrinsic property of TCR and not of the T cell expressing it and that there exist CD8-independent TCRs that have low or moderate affinity for their cognate ligands (37). One explanation for this is that CD8-independent TCRs bind their ligands in an orientation that disfavors efficient co-engagement of CD8 for steric reasons (38).

CD8β has been shown to play an important role in the thymic selection of CD8+ T cells (13–15, 39). Similar, albeit less

mice were incubated *in vitro* for 72 h with the indicated concentrations of GP33–41 peptides (KAVYNFATA). The proliferation of CD8+ T cells was assessed by flow cytometry. The bars indicate the proportion of undivided cells. One out of three experiments is shown. (D) The experiment was repeated using the weak peptide agonist GP33–41 Y4A (KAVANFATA). One out of two experiments is shown.

severe, effects were observed in mice expressing tailless CD8β (40). Remarkably, the impact of disruption of the CD8β gene or over-expression of tailless CD8β on thymic selection seems to depend on the Tg TCR that is used. For example, CD8 single-positive (SP) T cells were barely selected in CD8β-deficient H-Y TCR Tg mice (13). The selection of H-Y TCR^+ $CD4^-$ CD8+ thymocytes was also strongly compromised in mice expressing tailless CD8β, whereas the selection of F5 TCR Tg CD8+ thymocytes was not (40). We found that in P14 TCR transgenic mice, CD8β deficiency caused only a 2- to 3-fold reduction of peripheral CD8+ T cells (Fig. 6A and B and Supplementary Figure S2A, available at *International Immunology* Online). These findings argue that CD8β deficiency (or taillessness) affects the thymic selection of CD8+ T cells expressing CD8-dependent TCR more than those expressing CD8-independent TCR. This would imply that the TCR repertoire in naive CD8β KO mice is skewed toward CD8-independent specificities, i.e. should contain more CD8-independent CD8+ T cells than WT mice. This view is consistent with the marked differences observed in the TCRβ chain repertoire of naive B6 and CD8α KO mice (16, 17). On splenocytes from naive CD8β KO and B6 mice, we observed only scant differences in the TCR Vβ usage (Fig. 5B). However, if the diversity of the TCRβ chain repertoire in CD8β KO mice was similarly large as reported for B6 mice, our crude analysis would be prone to miss differences (25, 41).

Our results strongly suggested that the TCRα chain repertoire in CD8β KO and B6 mice is large because strong differences in TCR Vα usage became only apparent after gating on given Vβ (Fig. 5C–F). Moreover and importantly, disruption of the CD8β gene seems to strongly impact on the TCRα chain repertoire. Rearrangement of TCRα chains takes place on double-positive (DP) thymocytes and is terminated when a newly formed TCR together with CD8 provides a signal upon recognition of MHC I–peptide ligands on the thymic epithelium (39, 42, 43). Compromising CD8 by deletion of CD8β can be expected to impede this TCRαβ selection and therefore TCRα chain rearrangement to continue, until a TCR is formed that can provide a signal with CD8αα. This view is supported by several converging evidences, such as the following: (i) in CD8β-deficient, but not in normal, P14 TCR Tg mice, a high proportion of CD8+ T cells expressed in addition to the Tg P14 TCRα chain rearranged endogenous TCRα chains (Fig. 6A and B). These endogenously rearranged TCRα chains allowed selection of CD4+ T cells, expressing various levels of P14 TCR (Fig. 6A and B). (ii) The message for RAG1 in DP thymocytes from P14 × CD8β KO mice was ~10-fold higher than in DP thymocytes from P14 Tg mice (unpublished data). (iii) Due to hampered TCRαβ selection in CD8β KO and to a lesser extent in P14 × CD8β KO mice, the numbers of CD8 SP thymocytes and CD8+ T cells were reduced and those of CD4 SP thymocytes and CD4+ T cells increased (Supplementary Figure S2A, available at *International Immunology* Online).

Moreover, several observations argue that in CD8β (and CD8α) KO mice, TCRs of different affinities and sequences are selected and expanded upon viral infections than in B6 mice. For example, it has been demonstrated that high affinity MHC I–peptide ligands negatively select DP thymocytes in OT-1 TCR Tg mice, but positively select in CD8α-deficient OT-1 mice (42). This argues that CD8αβ lowers the affinity requirements for thymic selection, i.e. that in the absence of CD8β (and CD8α) the affinity windows for positive and negative selection are shifted to higher affinities (16, 44). This view is supported by the findings that (i) CD8β (and CD8α) KO and B6 mice exhibited differences in TCR repertoires of naive and virus-specific effector T cells (Fig. 5A–D, 16, 17) and (ii) GP33-specific CTL in CD8β (and CD8α) KO mice bound D^b-GP33 tetramer more avidly than CTL from B6 mice (Fig. 4E and F, 16).

Taken collectively, the present study demonstrates that CD8β KO mice can generate highly reactive primary, secondary and memory CD8+ T cell responses upon acute viral infections. It provides evidence that CD8β deficiency impacts on the TCRα chain rearrangement and the selection of the TCR repertoire, which allows preferential selection and expansion of CD8-independent TCR upon viral infection, which effectively compensates for the reduced co-receptor function of CD8αα.

Supplementary data

Supplementary figures are available at *International Immunology* Online.

Funding

Swiss National Foundation (no. 310000-108251).

Acknowledgements

We are grateful to M. Bachmann for providing GP33-VLPs, to A. Shamshiev for expert assistance with influenza infections, J. L. Maryanski, H. R. MacDonald, I. Ferrero and M. Kopf for helpful discussions, help and advise and to D. Dojcinovic and G. Bosshard for expert technical assistance.

Abbreviations

CFSE	5-(and-6)-carboxyfluorescein diacetate succinimidyl ester
d8	8 days
D^b-GP33	D^b loaded with GP33 peptide
D^b226/227-GP33	D^b mutant at residues 226 and 227 loaded with GP33 peptide
DP	double-positive
iv	intravenously
KO	knock out
LCMV	lymphocytic choriomeningitis virus
NP	nucleoprotein
RAG	recombinase activating genes
sc	subcutaneously
SP	single-positive
Tg	transgenic
VLP	virus-like particle
VSV	vesicular stomatitis virus
WT	wild type

References

1 Ledbetter, J. A., Seaman, W. E., Tsu, T. T. and Herzenberg, L. A. 1981. Lyt-2 and lyt-3 antigens are on two different polypeptide subunits linked by disulfide bonds. Relationship of subunits to T cell cytolytic activity. *J. Exp. Med.* 153:1503.

2 Moebius, U., Kober, G., Griscelli, A. L., Hercend, T. and Meuer, S. C. 1991. Expression of different CD8 isoforms on distinct human lymphocyte subpopulations. *Eur. J. Immunol.* 21:1793.

3 Cheroutre, H. and Lambolez, F. 2008. Doubting the TCR coreceptor function of CD8alphaalpha. *Immunity* 28:149.

4 Veillette, A., Bookman, M. A., Horak, E. M. and Bolen, J. B. 1988. The CD4 and CD8 T cell surface antigens are associated with the internal membrane tyrosine-protein kinase p56lck. *Cell* 55:301.
5 Devine, L., Kieffer, L. J., Aitken, V. and Kavathas, P. B. 2000. Human CD8 beta, but not mouse CD8 beta, can be expressed in the absence of CD8 alpha as a beta beta homodimer. *J. Immunol.* 164:833.
6 Wheeler, C. J., von Hoegen, P. and Parnes, J. R. 1992. An immunological role for the CD8 beta-chain. *Nature* 357:247.
7 Renard, V., Romero, P., Vivier, E., Malissen, B. and Luescher, I. F. 1996. CD8 beta increases CD8 coreceptor function and participation in TCR-ligand binding. *J. Exp. Med.* 184:2439.
8 Karaki, S., Tanabe, M., Nakauchi, H. and Takiguchi, M. 1992. Beta-chain broadens range of CD8 recognition for MHC class I molecule. *J. Immunol.* 149:1613.
9 Bosselut, R., Zhang, W., Ashe, J. M. *et al.* 1999. Association of the adaptor molecule LAT with CD4 and CD8 coreceptors identifies a new coreceptor function in T cell receptor signal transduction. *J. Exp. Med.* 190:1517.
10 Luescher, I. F., Vivier, E., Layer, A. *et al.* 995. CD8 modulation of T-cell antigen receptor-ligand interactions on living cytotoxic T lymphocytes. *Nature* 373:353.
11 Arcaro, A., Gregoire, C., Bakker, T. R. *et al.* 2001. CD8beta endows CD8 with efficient coreceptor function by coupling T cell receptor/CD3 to raft-associated CD8/p56(lck) complexes. *J. Exp. Med.* 194:1485.
12 Irie, H. Y., Mong, M. S., Itano, A. *et al.* 998. The cytoplasmic domain of CD8 beta regulates Lck kinase activation and CD8 T cell development. *J. Immunol.* 161:183.
13 Crooks, M. E. and Littman, D. R. 1994. Disruption of T lymphocyte positive and negative selection in mice lacking the CD8 beta chain. *Immunity* 1:277.
14 Fung-Leung, W. P., Kundig, T. M., Ngo, K. *et al.* 1994. Reduced thymic maturation but normal effector function of CD8+ T cells in CD8 beta gene-targeted mice. *J. Exp. Med.* 180:959.
15 Nakayama, K., Nakayama, K., Negishi, I. *et al.* 1994. Requirement for CD8 beta chain in positive selection of CD8-lineage T cells. *Science* 263:1131.
16 Riddle, D. S., Miller, P. J., Vincent, B. G. *et al.* 2008. Rescue of cytotoxic function in the CD8alpha knockout mouse by removal of MHC class II. *Eur. J. Immunol.* 38:1511.
17 Andrews, N. P., Pack, C. D. and Lukacher, A. E. 2008. Generation of antiviral major histocompatibility complex class I-restricted T cells in the absence of CD8 coreceptors. *J. Virol.* 82:4697.
18 Cawthon, A. G. and Alexander-Miller, M. A. 2002. Optimal colocalization of TCR and CD8 as a novel mechanism for the control of functional avidity. *J. Immunol.* 169:3492.
19 Fahmy, T. M., Bieler, J. G., Edidin, M. and Schneck, J. P. 2001. Increased TCR avidity after T cell activation: a mechanism for sensing low-density antigen. *Immunity* 14:135.
20 Manjunath, N., Shankar, P., Wan, J. *et al.* 2001. Effector differentiation is not prerequisite for generation of memory cytotoxic T lymphocytes. *J. Clin. Invest.* 108:871.
21 Sun, J. C. and Bevan, M. J. 2003. Defective CD8 T cell memory following acute infection without CD4 T cell help. *Science* 300:339.
22 Mercado, R., Vijh, S., Allen, S. E., Kerksiek, K., Pilip, I. M. and Pamer, E. G. 2000. Early programming of T cell populations responding to bacterial infection. *J. Immunol.* 165:6833.
23 van Stipdonk, M. J., Lemmens, E. E. and Schoenberger, S. P. 2001. Naive CTLs require a single brief period of antigenic stimulation for clonal expansion and differentiation. *Nat. Immunol.* 2:423.
24 Kaech, S. M. and Ahmed, R. 2001. Memory CD8+ T cell differentiation: initial antigen encounter triggers a developmental program in naive cells. *Nat. Immunol.* 2:415.
25 Blattman, J. N., Sourdive, D. J., Murali-Krishna, K., Ahmed, R. and Altman, J. D. 2000. Evolution of the T cell repertoire during primary, memory, and recall responses to viral infection. *J. Immunol.* 165:6081.
26 Masopust, D., Murali-Krishna, K. and Ahmed, R. 2007. Quantitating the magnitude of the lymphocytic choriomeningitis virus-specific CD8 T-cell response: it is even bigger than we thought. *J. Virol.* 81:2002.
27 Puglielli, M. T., Zajac, A. J., van der Most, R. G. *et al.* 2001. *In vivo* selection of a lymphocytic choriomeningitis virus variant that affects recognition of the GP33-43 epitope by H-2Db but not H-2Kb. *J. Virol.* 75:5099.
28 van der Most, R. G., Murali-Krishna, K., Whitton, J. L. *et al.* 998. Identification of Db- and Kb-restricted subdominant cytotoxic T-cell responses in lymphocytic choriomeningitis virus-infected mice. *Virology* 240:158.
29 Brändle, D., Brduscha-Riem, K., Hayday, A. C., Owen, M. J., Hengartner, H. and Pircher, H. 1995. T cell development and repertoire of mice expressing a single T cell receptor alpha chain. *Eur. J. Immunol.* 25:2650.
30 Angelov, G. S., Guillaume, P., Cebecauer, M. *et al.* 2006. Soluble MHC-peptide complexes containing long rigid linkers abolish CTL-mediated cytotoxicity. *J. Immunol.* 176:3356.
31 Durairaj, M., Sharma, R., Varghese, J. C. and Kane, K. P. 2003. Requirement for Q226, but not multiple charged residues, in the class I MHC CDloop/D strand for TCR-activated CD8 accessory function. *Eur. J. Immunol.* 33:676.
32 Boyman, O., Purton, J. F., Surh, C. D. and Sprent, J. 2007. Cytokines and T-cell homeostasis. *Curr. Opin. Immunol.* 19:320.
33 Wherry, E. J., Teichgraber, V., Becker, T. C. *et al.* 2003. Lineage relationship and protective immunity of memory CD8 T cell subsets. *Nat. Immunol.* 4:225.
34 Barber, D. L., Wherry, E. J. and Ahmed, R. 2003. Cutting edge: rapid *in vivo* killing by memory CD8 T cells. *J. Immunol.* 171:27.
35 Schwarz, K., Meijerink, E., Speiser, D. E. *et al.* 2005. Efficient homologous prime-boost strategies for T cell vaccination based on virus-like particles. *Eur. J. Immunol.* 35:816.
36 Kerry, S. E., Buslepp, J., Cramer, L. A. *et al.* 2003. Interplay between TCR affinity and necessity of coreceptor ligation: high-affinity peptide-MHC/TCR interaction overcomes lack of CD8 engagement. *J. Immunol.* 171:4493.
37 McNicol, A. M., Bendle, G., Holler, A. *et al.* 2007. CD8alpha/alpha homodimers fail to function as co-receptor for a CD8-dependent TCR. *Eur. J. Immunol.* 37:1634.
38 Buslepp, J., Wang, H., Biddison, W. E., Appella, E. and Collins, E. J. 2003. A correlation between TCR Valpha docking on MHC and CD8 dependence: implications for T cell selection. *Immunity* 19:595.
39 Bosselut, R., Kubo, S., Guinter, T. *et al.* 000. Role of CD8beta domains in CD8 coreceptor function: importance for MHC I binding, signaling, and positive selection of CD8+ T cells in the thymus. *Immunity* 12:409.
40 Itano, A., Cado, D., Chan, F. K. and Robey, E. 1994. A role for the cytoplasmic tail of the beta chain of CD8 in thymic selection. *Immunity* 1:287.
41 Lin, M. Y. and Welsh, R. M. 1998. Stability and diversity of T cell receptor repertoire usage during lymphocytic choriomeningitis virus infection of mice. *J. Exp. Med.* 188:1993.
42 Goldrath, A. W., Hogquist, K. A. and Bevan, M. J. 1997. CD8 lineage commitment in the absence of CD8. *Immunity* 6:633.
43 Kersh, G. J. 2004. Transcriptional control of thymocyte positive selection. *Immunol. Res.* 29:125.
44 Daniels, M. A., Teixeiro, E., Gill, J. *et al.* 2006. Thymic selection threshold defined by compartmentalization of Ras/MAPK signalling. *Nature* 444:724.